Acta Oceanol. Sin., 2023, Vol. 42, No. 9, P. 62–70
https://doi.org/10.1007/s13131-023-2157-y
http://www.aosocean.com
E-mail: ocean2@hyxb.org.cn

Geological context and vents morphology in the ultramafic-hosted Tianxiu field, Carlsberg Ridge

Jin Liang[1, 2], Chunhui Tao[1, 2, 3*], Xiangxin Wang[4*], Cheng Su[5], Wei Gao[4], Yadong Zhou[2], Weikun Xu[4], Xiaohe Liu[1, 6], Zhongjun Ding[4]

[1] Key Laboratory of Submarine Geosciences, Ministry of Natural Resources, Hangzhou 310012, China

[2] Second Institute of Oceanography, Ministry of Natural Resources, Hangzhou 310012, China

[3] School of Oceanography, Shanghai Jiao Tong University, Shanghai 200030, China

[4] National Deep Sea Center, Qingdao 266237, China

[5] School of Earth Sciences, Zhejiang University, Hangzhou 310027, China

[6] Ocean College, Zhejiang University, Zhoushan 316021, China

Received 26 August 2022; accepted 1 November 2022

Abstract

The Tianxiu hydrothermal field (TXHF) located on Carlsberg Ridge is one of the few active ultramafic-hosted venting systems known in the Indian Ocean. Despite numerous investigations, there is limited understanding of its sulfide structure morphology, and the factors controlling the formation of TXHF are poorly understood. In this study, we conducted detailed seafloor mapping using visual data obtained by dives using the human-occupied vehicle (HOV) *Jiaolong*. The TXHF is found to be an active, off-axis, ultramafic-hosted, high-temperature hydrothermal area in which serpentine peridotite is exposed. Two main hydrothermal sites were identified, i.e., P and Y, both of which feature a complex of chimneys and beehive diffusers constituting a "chimney jungle" and isolated large steep-sided structures developed on flat-lying sulfide mounds. In addition, some sporadic inactive chimneys and outcrops of hydrothermal deposits were noted. The chimneys are rich in Fe and Zn sulfide, and lack the central fluid channel formed by focused high-temperature fluid flow. Hydrothermal venting at TXHF is likely related to low-angle detachment faults that focus and transport hydrothermal fluids away from a heat source along the valley wall. Our results complement and expand upon previous works concerning sulfide chimney morphology and their corresponding mineral paragenesis in ultramafic-hosted hydrothermal systems in the Indian Ocean and further our understanding of modern seafloor hydrothermal systems.

Key words: hydrothermal activity, sulfide accumulation, morphology, ultramafic-hosted, Carlsberg Ridge

Citation: Liang Jin, Tao Chunhui, Wang Xiangxin, Su Cheng, Gao Wei, Zhou Yadong, Xu Weikun, Liu Xiaohe, Ding Zhongjun. 2023. Geological context and vents morphology in the ultramafic-hosted Tianxiu field, Carlsberg Ridge. Acta Oceanologica Sinica, 42(9): 62–70, doi: 10.1007/s13131-023-2157-y

1 Introduction

Diverse active hydrothermal systems have been documented along mid-ocean ridges, volcanic arcs, and in back-arc basins (Baker, 2017; Beaulieu et al., 2015; Hannington et al., 2005). Seafloor massive sulfides are major products of hydrothermal activity and are rich in elements such as Fe, Cu, Zn, Au, and Ag. In addition to their significance as potential future metal resources (Hannington et al., 2011), hydrothermal systems provide critical constraints on material and energy exchanges among the lithosphere, hydrosphere, and biosphere (Alt, 1995; de Ronde et al., 2005; Kelley et al., 2002; Tivey, 2007; Von Damm, 1995). The formation and evolution of modern seafloor hydrothermal systems have drawn increased interest during the last half century (Barreyre et al., 2012; Fouquet et al., 1996; Genna et al., 2014; Haymon, 1983; Ludwig et al., 2006; Meng et al., 2019; Von Damm et al., 1997). Understanding the factors that control the distribution and type of hydrothermal venting is key to developing tools for seafloor exploration and exploiting the metallogenic potential of ancient massive sulfide deposits using modern analogues (Hannington et al., 2005).

The Indian Ocean Ridges are up to approximately 18 000 km in length, with various full spreading rates (<12–60 mm/a). Exploration of hydrothermal activity along these ridges has identified a series of extinct sites and seawater anomalies (German et al., 1998; Halbach et al., 1998; Münch et al., 2000); the first direct observations of an active hydrothermal field in the Indian Ocean was at Kairei in 2000 (Gamo et al., 2001) and the first high-temperature venting field was confirmed along the ultraslow-spreading Southwest Indian Ridge in 2007 at Longqi (Tao et al., 2012). Subsequent exploration efforts along the Southwest, Central (and the Carlsberg) and Southeast Indian Ridges visually identified more than twenty active and extinct vent sites, and numerous seawater anomalies have been located. They may be controlled by geologic settings and diverse hydrothermal circulation pro-

Foundation item: The National Key Research and Development Program of China under contract No. 2017YFC0306603; the Scientific Research Fund of the Second Institute of Oceanography, Ministry of Natural Resources under contract Nos JG1905 and SZ2201; the National Natural Science Foundation of China under contract No. 41806076; and the National Key Research and Development Program of China under contract No. 2021YFC2801705.

*Corresponding author, E-mail: taochunhuimai@163.com; wangxiangxin@ndsc.org.cn

cesses, and play host to unique ecologic communities (Van Dover et al., 2001; Zhou et al., 2022) and form hydrothermal deposits in various morphology, some of which could be of great economic potential of mineral resources (Yu et al., 2021).

Wang et al. (2021) summarized the occurrences of hydrothermal sulfide fields in the Indian Ocean into two groups. Unlike the slow-spreading Mid-Atlantic Ridge (MAR) (Fouquet et al., 2010), relatively few sulfide deposits along the length of the Indian Ocean Ridges occurred off-axis high on the rift valley wall, either hosted by or related to ultramafic rocks (e.g., Tianzuo, Onnuri, Cheoeum, Yokoniwa, and Tianxiu) (Table 1). Previous research concerning the mineralization and hydrothermal processes of these deposits has been restricted to extinct or waning systems (Choi et al., 2021; Ding et al., 2021, 2022; Lim et al., 2022). The ultramafic-hosted Tianxiu hydrothermal field (TXHF) (3.70°N, 63.83°E, water depth about 3 350 m) is located on slow-spreading Carlsberg Ridge (CR), first documented during the 26th Chinese Cruise in 2012, which conducted a plume survey (Tao et al., 2013). The TXHF was visually confirmed in 2015 during the 33rd cruise (Jiang et al., 2015), and further investigated by video reconnaissance using the human-occupied vehicle (HOV) *Jiaolong*. In 2017 (cruise report of Chinese Dayang Cruise 38th, National Deep Sea Center, 2017), coupled with high-resolution bathymetric side scan mapping. Further *Jiaolong* dives were devoted to the TXHF in 2022 (Chinese Dayang Cruise 72nd), and based on this cruise, this paper describes the distribution and characteristics of hydrothermal activity at this location and discusses the geological factors controlling the TXHF.

2 Geological setting

The CR is a slow-spreading ridge with a full spreading rate of 22–32 mm/a (Raju et al., 2008). It extends from 2°S to 10°N and forms the northern section of the Central Indian Ridge (CIR) in the western Indian Ocean, connecting the African and Indo–Australian plates. The first major evidence of hydrothermal activity at the CR was the observation of an event plume, recorded by conductivity-temperature-depth (CTD) measurements and Miniature Autonomous Plume Recorder casts in 2003 (Murton et al., 2006). Three active hydrothermal fields have been reported along the CR, i.e., the Wocan-1, Daxi, and Tianxiu fields (Qiu et al., 2021; Wang et al., 2021), and sediments from the ridge flank and cores have been found to contain hydrothermal components with Mn and Fe contents up to 44.63 wt% and 26.95 wt%, respectively (Olatunde and Akintoye, 2021).

The TXHF is located on the southern valley wall of the ridge axis at a water depth of 3 300–3 500 m (Fig. 1). It is the first confirmed high-temperature active ultramafic-hosted hydrothermal system in the Indian Ocean. Its location on the northwestern slope of an oceanic core mosaic lies approximately 5 km away from the ridge axis (Yang et al., 2021a), and peridotites in the area have undergone extensive serpentinization (Chen et al., 2020). The surface sediments show a dominance of Cu-Zn-Fe (equiaxial cubanite, cubanite, sphalerite and pyrrhotite) sulfide aggregates in samples collected adjacent to the vent area, whereas fine-grained Fe-oxides and hydroxides and calcite were found outside the hydrothermal field (Cai et al., 2020).

3 Data and methods

Ship-based bathymetric data of the study area were newly acquired using a Kongsberg EM124 multibeam system during research Chinese Dayang Cruise 72nd in 2022. Additional bathymetric data and side scan sonar data of the hydrothermal area were obtained using the high-resolution bathymetric side-scan sonar (HRBSSS) system of the manned submersible *Jiaolong* which surveyed ~80 m above the seafloor at a speed of less than 2 kn. The pulse length of the HRBSSS sonar was 6 ms, with a maximum ping rate of 2 Hz, and a center frequency of approximately 150 kHz. The sonar beam opening angle of 100° (both sides, across track) and 1.5° along track allowed for maximum coverage width of sounding is 500 m and maximum coverage width of side scan is 800 m. Underwater acoustic communication devices transmitted positioning data obtained by a POSIDONIA USBL on the R/V *Shenhaiyihao*, allowing for the determination of the initial position of the integrated navigation system. The Doppler Velocity Log mounted on the submersible provided information on the velocity over ground. Motion sensor IXBLUE Octans provided data on attitude and heading. Both datasets were used to supplement HRBSSS data to aid navigation. The CTD installed on the submersible provided depth and sound velocity information. Final data cleaning of the positions and the mosaicking of the im-

Table 1. Ultramafic-hosted or related hydrothermal fields reported in the Indian Ocean

Site	Location	Latitude	Longitude	Water depth/m	Full spreading rate/ (mm·a^{-1})	Activity	Host rock	Tectonica control	Deposit of mineralization	Source
Tianxiu	CR	3.70°N	63.83°E	3 350	24.5	active	ultramafic rocks	detachment fault	chimney, mound	this study
Onnuri	CIR	11.42°S	66.42°E	2 000	34.4	diffuse	ultramafic rocks	detachment fault	breccia	Lim et al. (2022)
Cheoeum	CIR	12.67°S	66.20°E	3 100	36.7	diffuse	ultramafic rocks	oceanic core complexes	chimney, mound	Choi et al. (2021)
Yokoniwa	CIR	25.27°S	70.07°E	2 500	47.2	inactive	ultramafic rocks	non-transform offset	small sulfide chimneys	Fujii et al. (2016)
Kairei	CIR	25.32°S	70.03°E	2 450	47.5	active	basalt	detachment fault	mound, chimeny, massive sulfide, breccia	Nakamura et al. (2009) Wang et al. (2018)
Tianzuo	SWIR	27.95°S	63.53°E	3 630	12	inactive	ultramafic rocks	detachment fault	breccia, mound	Ding et al. (2021)
Longqi	SWIR	37.78°S	49.65°E	2 700	14	active	basalt	detachment fault	mound, chimeny, massive sulfide, breccia	Tao et al. (2014)
Yuhuang	SWIR	37.94°S	49.26°E	1 500	14	inactive	basalt	detachment fault	massive sulfide, breccia	Yu et al. (2021)

Note: CR: Carlsberg Ridge; CIR: Central Indian Ridge; SWIR: Southwest Indian Ridge.

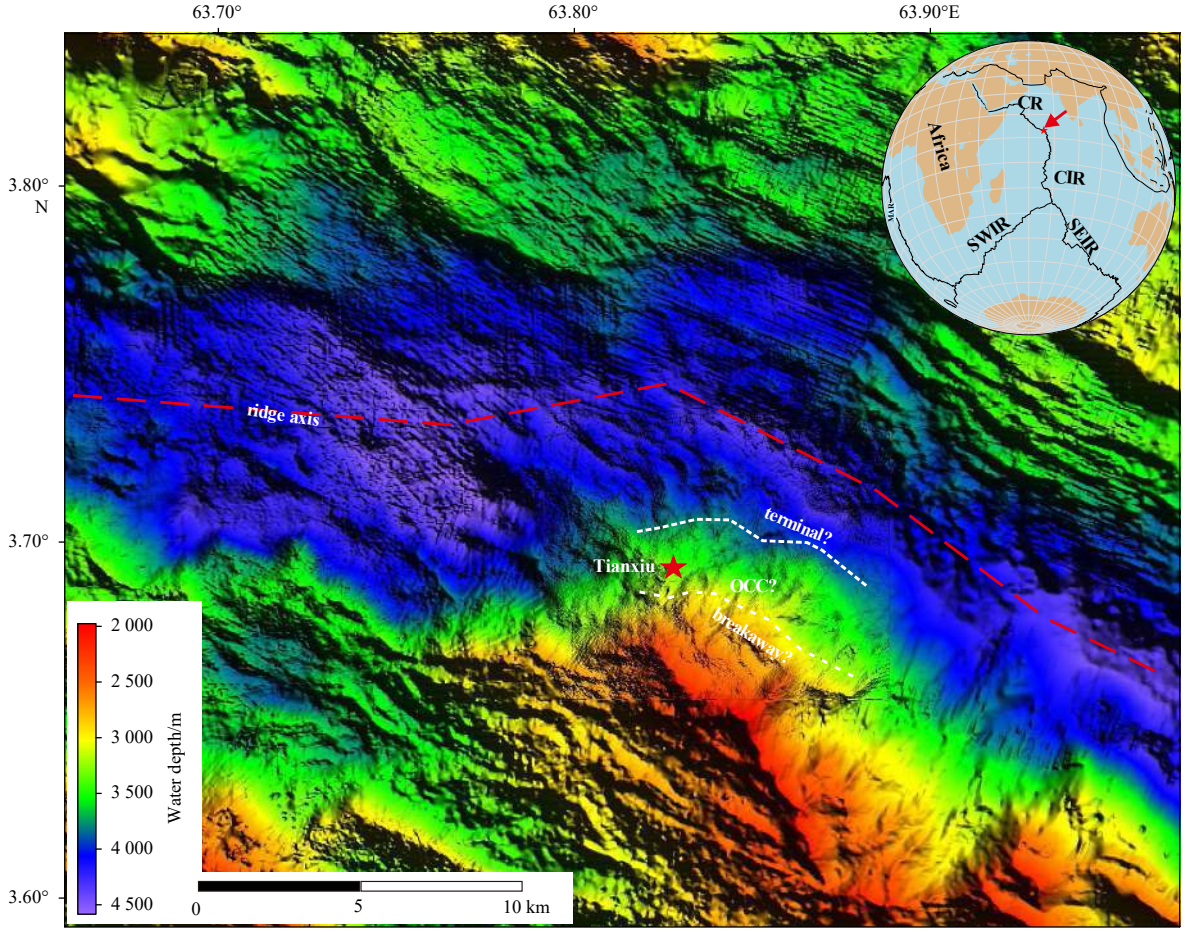

Fig. 1. Bathymetric map of the Tianxiu hydrothermal field on the Carlsberg Ridge (CR) (the bathymetric data were collected by multibeam surveys of Chinese Dayang Cruise in 2013). The red dashed line indicates the ridge axis. CIR: Central Indian Ridge; SWIR: Southwest Indian Ridge; SEIR: Southeast Indian Ridge. OCC: Oceanic Core Complex.

ages were conducted using the CleanSweep3 seafloor mapping software developed by Oceanic Imaging Consultants, Inc (Yang et al., 2021b). For near-bottom optical surveys, the submersible is equipped with a 3CCD TV (charged coupled device television) camera with parallel laser scale (0.1 m spacing), eight lights, two 1CCD TV cameras, and a pan-and-tilt digital still camera. Still images and high-definition video footage were used to create image mosaics following the methods adopted by Sheng et al. (2020). Geological samples were collected using the manipulator of the submersible *Jiaolong* in the Chinese Dayang Cruise 72nd.

4 Results and discussion

4.1 *Observation of the Tianxiu vent field*

Fragments of serpentinized peridotite were widely observed in and around the Tianxiu Hydrothermal Field (TXHF) (Fig. 2d), and evidence of faults was also obvious, including scratches and steps (Fig. 2e). Outcrops of mylonitized peridotite were observed (Fig. 2f). Nearly E–W fractures/fissures and landslides were commonly distributed, and hydrothermal products were identified along the fractures/fissures (Figs 2g, h). Sediments were found to be widely distributed, and inactive chimneys could be seen exposed throughout pelagic sediments (Fig. 2h). The pelagic sediments in the southeast of the hydrothermal area have a thickness of more than 50 cm (Fig. 2i), and wave markings were rarely observed.

With the exception of sporadic inactive chimneys and outcrops of hydrothermal deposits, hydrothermal chimneys were found to be concentrated in the Yu (Y) and Pan flut (P) sites sites, which are approximately 200 m apart (Fig. 2a). The Y site is located at a water depth of 3 370 m, with continuously visible hydrothermal deposits over a range of ~30 m. Numerous slender beehive-like chimneys 10–50 cm in diameter aggregate into a huge steep-sided structure ~5 m in diameter and ~18 m in height (Fig. 3a). At the top of the Y structure, vigorous black smoke indicating active high-temperature venting was observed (Fig. 3b), and a large number of beehive diffusers with brownish Fe-oxide surface coatings and slowly venting clear hydrothermal fluids can be seen in the middle of the structure (temperature measured at 210–270℃ in Chinese Dayang Cruise 72nd) (Fig. 3c). An obvious horizontal boundary between the brownish sulfide base and the dark gray active chimney can be seen at the bottom of this structure (Fig. 3d), and massive sulfide and chimney fragments are distributed at the foot (Fig. 3e). The Y site is characterized by an extremely high density of alvinocaridid shrimps (Zhou et al., 2022), which predominantly gather in the active beehive chimneys (Figs 3a, c and d).

The P site is located at the north side at water depths of 3 320–3 365 m, extends for ~60 m from east to west and ~50 m from north to south, and can be identified in the bathymetric side scan images (Figs 2b, c). This site consists of a large number of chimneys with diameters of 10–50 cm and heights of 1–5 m following a NW–SE striking line, parallel to the strike of the vent field itself, forming a “chimney jungle” (Figs 3f, h and i). Com-

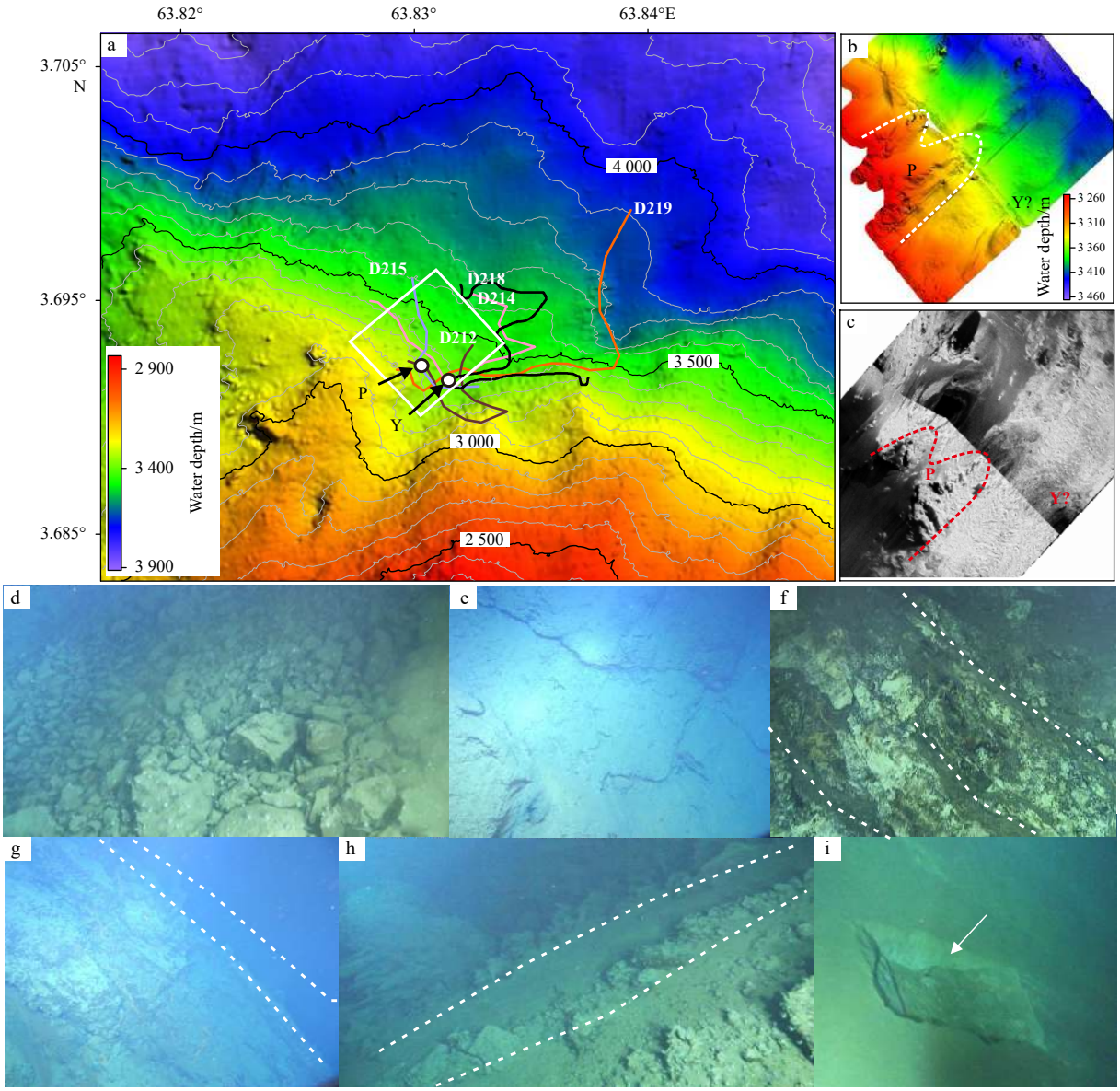

Fig. 2. Seafloor morphology of the Tianxiu hydrothermal field. Bathymetric map of the study area showing track of the submersible *Jiaolong*'s dives in Chinese Dayang Cruise 72nd, the white box shows the range of the side scan (the bathymetric data were collected by multi-beam surveys of Chinese Dayang Cruise 72nd in 2022) (a); colored and corresponding backscatter image showing the main area of the P site (white and red dashed lines, respectivelys) (b, c); scattered serpentine peridotite fragments (d); fault scratch and steps (e); mylonitized outcrop, white dotted line indicates the approximate strike of the fault (f); accumulation of hydrothermal deposits can be seen at the landslides (g); sulfide distributed in lines (h); pelagic sediments showing a certain thickness of more than 50 cm (the square pit is caused by box sampler) (i). All photos or videos were taken in Chinese Dayang Cruise 72nd in 2022.

pared with Y, the P site is significantly less active, as shown by the large number of upright, toppled chimney clusters with yellowish-brown oxides on the surface of the surrounding beehive diffusers. A small number of "flanges" were observed on this inactive structure (Figs 3f, g); such features are rare in ultramafic-hosted hydrothermal fields. Patches of *Alviniconcha marisindica* snails, accompanied by alvinocaridid shrimps and bathymodiolin mussels, dominated the faunal assemblages surrounding the diffusing beehive-like chimneys (Zhou et al., 2022), and anemones flourished in inactive areas of the P site (Fig. 3j).

4.2 *Formation of sulfide deposits*

The TXHF is one of few presently known hydrothermal areas associated with ultramafic rocks in the Indian Ocean (Table 1). Like other ultramafic-hosted high-temperature venting fields (Rainbow, Logatchev, and Ashadze), the discharge in the TXHF is less focused than others of mafic-hosted (Fouquet et al., 2010). However, peculiar features such as the "chimney jungle" at the P site and steep-sided structure at the Y site differ from most other seafloor hydrothermal systems. For example, the basalt-hosted hydrothermal deposits along the East Pacific Rise feature mainly individual chimneys (Hannington et al., 1995; Haymon and Kastner, 1981; Hekinian et al., 1985; Tivey et al., 1999); at Endeavour, mainly large steep-sided structures occur; those at Galapagos or Trans-Atlantic Geotraverse (TAG) are hydrothermal mounds; black smoker complexes with a maximum height of ~10 m occur in the Kairei vent area (Gallant and Von Damm, 2006); and 2–3 m tall, slender, focused black smoker chimneys characterize the

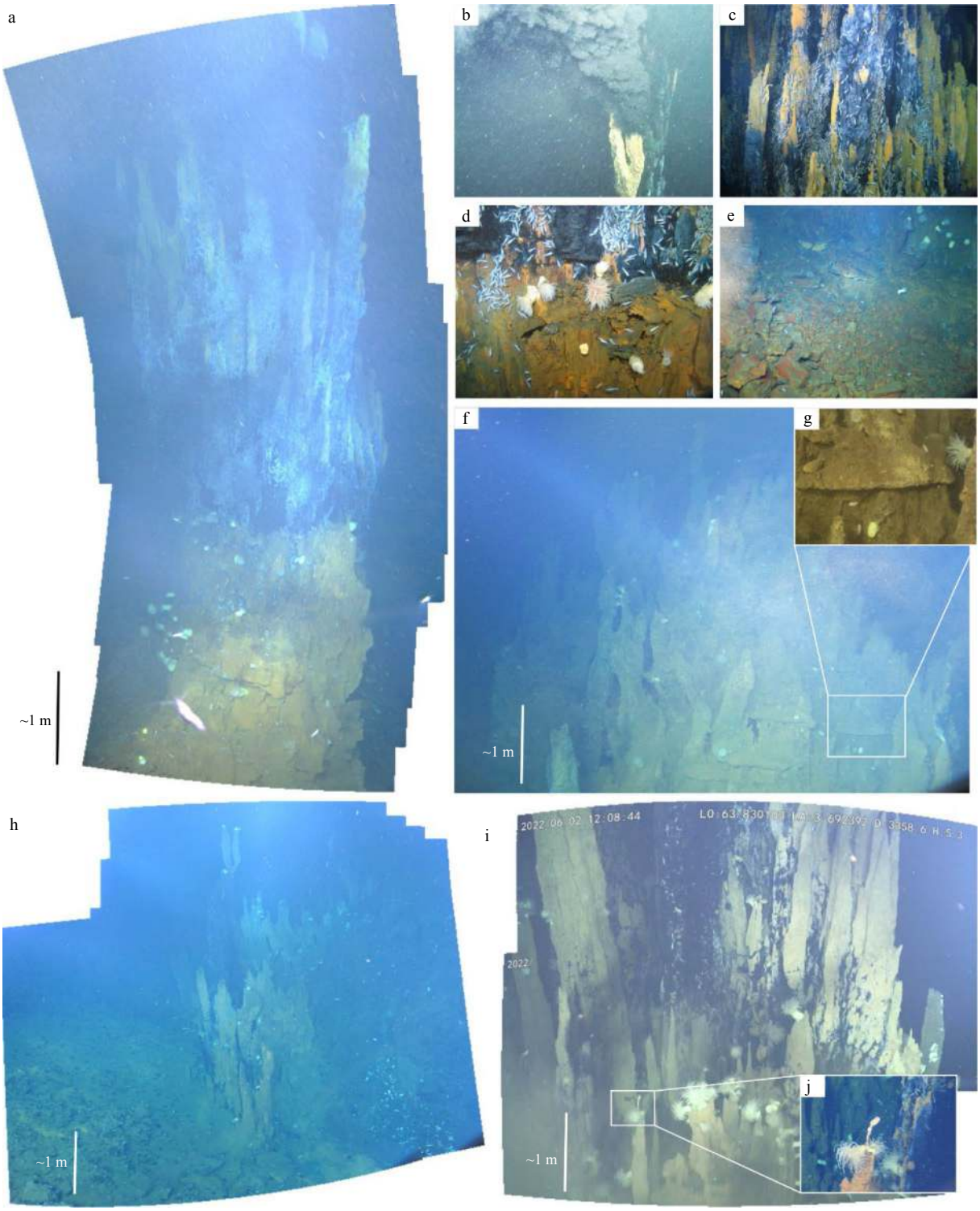

Fig. 3. Representative chimney morphology in Tianxiu hydrothermal field. Mosaic of the Y chimney (similar in shape to the Chinese classical folk instrument "Yu") (a); focused fluid flow emitting for the top of the Y structure (b); beehive structures at the middle of the Y structure showing dominance of alvinocaridid shrimps (c); the boundary between the brownish sulfide base and the dark-gray active chimneys (d); massive sulfide and chimney fragments at the foot of the Y site (e); inactive chimneys complex in P site (similar in shape to the Chinese classical folk instrument "Pan Flute" P) (f), showing small flanges with ~10 cm in width (g); lined distributed chimneys in P site showing white shells of mussels indicating waning stage (h); beehive diffusers shimmering light smoke surrounded by toppled chimney clusters in P site with yellowish-brown oxide on the surface (i), showing anemones and *Alviniconcha marisindica* snails (j). All photos or videos were taken in Chinese Dayang Cruise 72nd in 2022.

Beebe vents in the Mid-Cayman Rise (Kinsey and German, 2013). The TXHF also significantly differs from some representative ultramafic-hosted hydrothermal deposits along the Mid-Atlantic Ridge (MAR), where hydrothermal venting largely occurs

through smoking craters with a pronounced rim and a central depression that is a few meters deep, lacking large chimney structures (e.g., Logatchev-1, Ashadze, and Nibelungen) (Fouquet et al., 2008; Melchert et al., 2008; Petersen et al., 2009).

Regardless of their size and activity, the chimneys in the TXHF are mainly classified as beehive structures (Figs 4a, b). Beehive structures are a category of chimneys with more diffuse or lower flow velocities than focused chimney, first reported at the Snake Pit hydrothermal field on the MAR (Fouquet et al., 1993), such structures occur widely at other seafloor hydrothermal sites, such as Cleft, Logatchev, Beebe, Piccard, and NW Caldera (Berkenbosch et al., 2012; Kinsey and German, 2013; Koski et al., 1994; Petersen et al., 2009; Webber et al., 2017; Wheeler et al., 2013). Beehive diffusers in the TXHF share common features with other hydrothermal vent fields, such as lacking a principle axial fluid conduit (Koski et al., 1994; Webber et al., 2017). A cross-section of these beehive chimney shows porous concentric layers of Zn- and Fe-sulfide minerals (pyrrhotite, pyrite, and sphalerite) surrounding mini fluid conduits (Figs 4e–g), although some chimneys are Zn-sulfide rich (Fig. 4h); the principal difference between beehive and focused venting chimneys is their lack of central fluid conduits that are typically lined by inner zones of fine-to-coarse-grained chalcopyrite (Fig. 4i). Instead, the beehive diffuser structure has a highly porous axial zone through which fluids diffuse upward and laterally rather than passing through a principal axial conduit (Fouquet et al., 1993). Previous studies have proposed that beehive diffusers may be excellent carriers of high gold concentrations (Fouquet et al., 1993; Webber et al., 2017), and native Au in sulfides from TXHF has been preliminarily reported (Yang et al., 2021a), as they contain highly porous pyrrhotite framework, which indicate favorable highly reduced conditions for gold precipitation (Webber et al., 2017).

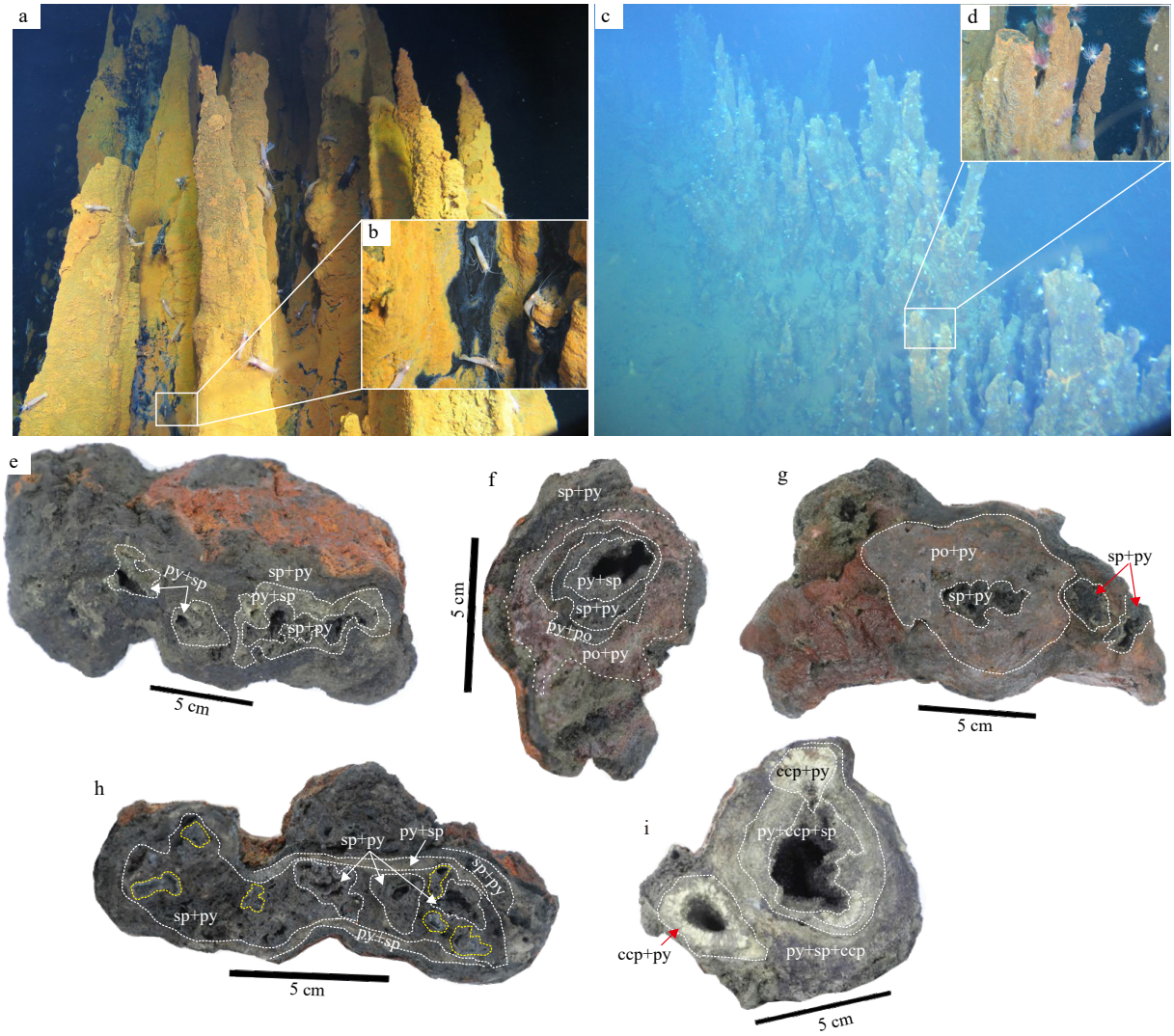

Fig. 4. Representative chimney fragments in Tianxiu hydrothermal field. a. Toppled chimney clusters in P site with yellowish-brown oxide on the surface, partly in dark gray (b), indicating status of still active. c. The extinct "chimney jungle" in P site, showing absence of large fluid conduit (d). e. Chimney fragment collected from Y site showing multi fluid conduits wall mainly composed of pyrite and sphalerite. f. Chimney fragment collected from Y site showing major fluid conduit wall mainly composed of pyrite and sphalerite, showing reddish-brown pyrrhotite rich layer. g. Another chimney fragment showing major reddish-brown pyrrhotite rich layer; h. Inactive chimney fragment collected from P site, showing sphalerite rich and multi micro fluid conduits. i. Chimney fragment of focused fluid flow, rich in chalcopyrite and pyrite composing the fluid conduit walls, collected from other high-temperature hydrothermal area is taken here for comparison. py: pyrite; sp: sphalerite; po: pyrrhotite; ccp: chalcopyrite. The scale bar represents 5 cm.

In addition, although the small size of the flange is far smaller than those at the Endeavour segment and Snake Pit field, where sulfide structures are dominated by flanges with high-temperature chimneys (Delaney et al., 1992; Robigou et al., 1993), the small flanges observed in the TXHF are rare but interesting phenomena in ultramafic-hosted hydrothermal areas. Delaney et al. (1992) presented a model for the outward growth of sulfide structures, wherein episodic shifts in the bulk permeability of the capping vent structure result in multiple tiers of flanges. The formation of flanges at the TXHF may indicate a decline in fault-controlled conduit permeability at the distal end, i.e., far from the ridge axis and close to the termination of the detachment fault.

4.3 *Indication to the subseafloor hydrothermal circulation*

In previous studies, the host rock has been proposed as the principal factor controlling variations in the morphology and size of hydrothermal deposits (Fouquet et al., 1993), for instance, a flat-lying profile corresponds to ultramafic basement, whereas a mound-like structure is commonly basalt-hosted (Fouquet et al., 2010). This viewpoint is supported by our seafloor investigations in the TXHF, where the "chimney jungle" at the P site and the steep-sided structure at the Y site both occur on relatively flat deposits. The construction of large-scale sulfide accumulations requires a long and steady period of hydrothermal fluid circulation. Mixing between fluid flows and seawater, the permeability of fluid conduits, and the stability of the hydrothermal system, among other factors, have been proposed as controls on the shape and scale of large-scale hydrothermal sulfide deposits (Haymon, 1983; Herzig and Hannington, 1995; Peng and Zhou, 2005; Tivey, 2007; You and Bickle, 1998). Morphological differences between the TXHF and other hydrothermal fields may reflect the geometry of the hydrothermal up flow and, especially, the permeability of the crust in the upper few hundred meters below the seafloor (Jamieson et al., 2017).

The most plausible reason for the differences in the internal morphologies observed at the P and Y sites in the TXHF is a combination of factors and local differences in subseafloor fluid pathways, similar to the different vent styles observed at the Logatchev-1 field (Petersen et al., 2009). Additionally, the widely observed beehive structures in the TXHF may indicate fluctuations in temperature and/or vent fluid composition (Webber et al., 2017). Bathymetric mapping, geological sampling and seafloor observations have suggested that hydrothermal venting at the TXHF is likely related to low-angle detachment faults that focus and transport hydrothermal fluids away from a heat source, likely mafic intrusions along the southern rift valley wall (Fig. 5). Fluids may pass through permeable layers in the subseafloor, where their diversion creates distinct vent sites and areas of diffuse venting. At the Y site, with more stable enhanced heat and limited mixing of seawater, focused fluid flow from the subsurface to the seafloor results in a large steep-sided structure that emanates black smoker fluids. At the P site, the enhanced mixing of seawater in the up-flow zone within or underneath the flat-lying mound may lead to conductive cooling and therefore lower vent fluid exit temperatures during the waning stage. Further sampling and dating are expected to determine whether venting was continuous or discontinuous at the TXHF.

5 Summary

In this study, we have described the morphology of hydrothermal structures throughout the TXHF, a typical ultramafic-hosted high-temperature active hydrothermal area, where outcrops of serpentine peridotite are exposed and where evidence of significant tectonic activities such as mylonitization is observed. Hydrothermal activities in the area are mainly distributed at the P and Y sites, which are approximately 200 m apart. These sites are characterized by "chimney jungles" and isolated steep-sided structures developed on flat-lying sulfide mounds. The chimneys are primarily beehive structures, rich in Fe and Zn sulfide, and lack the central fluid channel characteristic of focused high-temperature fluid flow. In addition, sporadic inactive chimneys and outcrops of hydrothermal deposits indicating past hydrothermal activities were observed. No significant differences were observed between the dominant vent biota in the TXHF and those

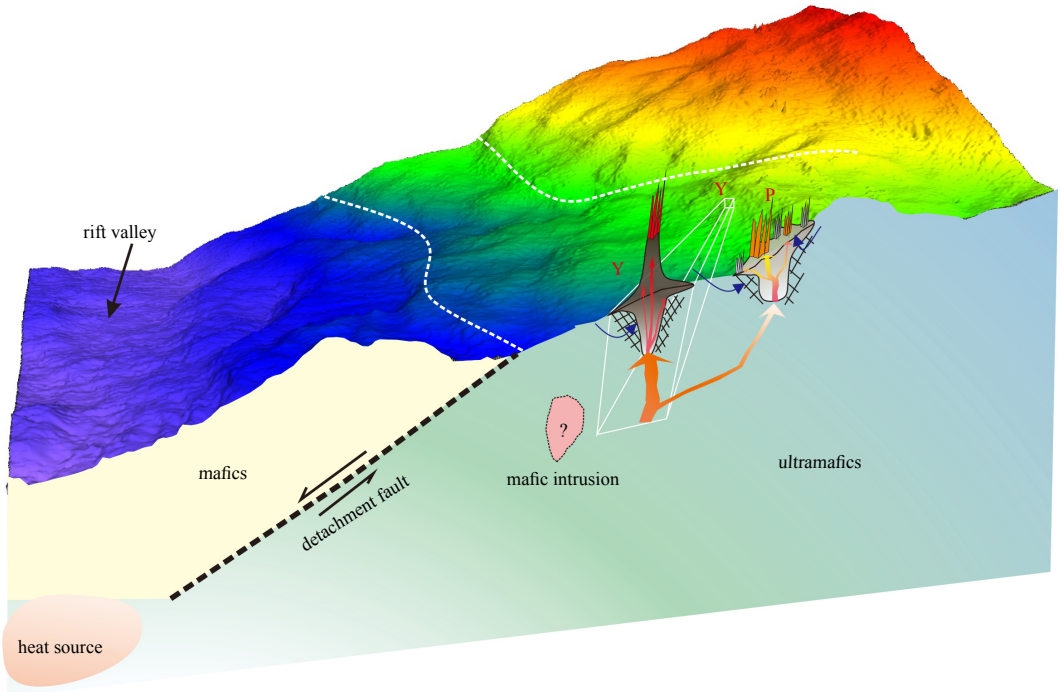

Fig. 5. Schematic model for fluid circulation at Tianxiu hydrothermal field.

in the CR and CIR. Hydrothermal venting at the TXHF is likely related to low-angle detachment faults focusing and transporting hydrothermal fluids away from a heat source along the valley wall. Further geological and geochemical characterization need to be conducted to better understand ultramafic-hosted hydrothermal mineralization in the Indian Ocean.

Acknowledgements

We thank captain and crew of the COMRA Cruise 72nd on R/V *Shenhaiyihao*. Special thanks go to the submersible *Jiaolong* group. The Daxi group lead by Xiqiu Han is specially thanked for intellectual support. We are also grateful for the constructive comments and suggestions from two anonymous reviewers.

References

Alt J C. 1995. Subseafloor processes in mid-ocean ridge hydrothennal systems. In: Humphris S E, Zierenberg R A, Mullineaux L S, et al., eds. Seafloor Hydrothermal Systems: Physical, Chemical, Biological, and Geological Interactions. Washington, DC: American Geophysical Union, 91: 85–114

Baker E T. 2017. Exploring the ocean for hydrothermal venting: New techniques, new discoveries, new insights. Ore Geology Reviews, 86: 55–69, doi: 10.1016/j.oregeorev.2017.02.006

Barreyre T, Escartín J, Garcia R, et al. 2012. Structure, temporal evolution, and heat flux estimates from the Lucky Strike deep-sea hydrothermal field derived from seafloor image mosaics. Geochemistry, Geophysics, Geosystems, 13(4): Q04007

Beaulieu S E, Baker E T, German C R. 2015. Where are the undiscovered hydrothermal vents on oceanic spreading ridges?. Deep-Sea Research Part II: Topical Studies in Oceanography, 121: 202–212, doi: 10.1016/j.dsr2.2015.05.001

Berkenbosch H A, De Ronde C E J, Gemmel J B, et al. 2012. Mineralogy and formation of black smoker chimneys from Brothers submarine volcano, Kermadec arc. Economic Geology, 107(8): 1613–1633, doi: 10.2113/econgeo.107.8.1613

Cai Yiyang, Han Xiqiu, Qiu Zhongyan, et al. 2020. Characteristics, distribution and implication of hydrothermal minerals in Tianxiu Hydrothermal Field, Carlsberg Ridge, Northwest Indian Ocean. Marine Geology & Quaternary Geology, 40(5): 36–45

Chen Yang, Han Xiqiu, Wang Yejian, et al. 2020. Precipitation of calcite veins in serpentinized harzburgite at Tianxiu hydrothermal field on carlsberg ridge (3.67°N), Northwest Indian Ocean: Implications for fluid circulation. Journal of Earth Science, 31(1): 91–101, doi: 10.1007/s12583-020-0876-y

Choi S K, Pak S J, Kim J, et al. 2021. Gold and tin mineralisation in the ultramafic-hosted Cheoeum vent field, Central Indian Ridge. Mineralium Deposita, 56(5): 885–906, doi: 10.1007/s00126-020-01012-5

de Ronde C E J, Hannington M D, Stoffers P, et al. 2005. Evolution of a submarine magmatic-hydrothermal system: Brothers volcano, southern Kermadec arc, New Zealand. Economic Geology, 100(6): 1097–1133, doi: 10.2113/gsecongeo.100.6.1097

Delaney J R, Robigou V, McDuff R E, et al. 1992. Geology of a vigorous hydrothermal system on the Endeavour Segment, Juan de Fuca Ridge. Journal of Geophysical Research: Solid Earth, 97(B13): 19663–19682, doi: 10.1029/92JB00174

Ding Teng, Tao Chunhui, Dias Á A, et al. 2021. Sulfur isotopic compositions of sulfides along the Southwest Indian Ridge: implications for mineralization in ultramafic rocks. Mineralium Deposita, 56(5): 991–1006, doi: 10.1007/s00126-020-01025-0

Ding Teng, Wang Jia, Tao Chunhui, et al. 2022. Trace-element compositions of sulfides from inactive Tianzuo hydrothermal field, Southwest Indian Ridge: Implications for ultramafic rocks hosting mineralization. Ore Geology Reviews, 140: 104421, doi: 10.1016/j.oregeorev.2021.104421

Fouquet Y, Cambon P, Etoubleau J, et al. 2010. Geodiversity of hydrothermal processes along the Mid-Atlantic Ridge and ultramafic-hosted mineralization: A new type of oceanic Cu-Zn-Co-Au volcanogenic massive sulfide deposit. In: Rona P A, Devey C W, Dyment J, eds. Diversity of Hydrothermal Systems on Slow Spreading Ocean Ridges. Washington, DC: American Geophysical Union, 188: 321–367

Fouquet Y, Cherkashov G, Charlou J L, et al. 2008. Serpentine cruise-ultramafic hosted hydrothermal deposits on the Mid-Atlantic Ridge: First submersible studies on Ashadze 1 and 2, Logatchev 2 and Krasnov vent fields. InterRidge News, 17: 16–21

Fouquet Y, Knott R, Cambon P, et al. 1996. Formation of large sulfide mineral deposits along fast spreading ridges. Example from off-axial deposits at 12°43′N on the East Pacific Rise. Earth and Planetary Science Letters, 144(1–2): 147–162, doi: 10.1016/0012-821X(96)00142-2

Fouquet Y, Wafik A, Cambon P, et al. 1993. Tectonic setting and mineralogical and geochemical zonation in the Snake Pit sulfide deposit (Mid-Atlantic Ridge at 23°N). Economic Geology, 88(8): 2018–2036, doi: 10.2113/gsecongeo.88.8.2018

Fujii M., Okino K., Sato T, et al. 2016. Origin of magnetic highs at ultramafic hosted hydrothermal systems: Insights from the Yokoniwa site of Central Indian Ridge. Earth & Planetary Science Letters, 441: 26–37

Gallant R M, Von Damm K L. 2006. Geochemical controls on hydrothermal fluids from the Kairei and Edmond Vent Fields, 23°–25°S, Central Indian Ridge. Geochemistry, Geophysics, Geosystems, 7(6): Q06018

Gamo T, Chiba H, Yamanaka T, et al. 2001. Chemical characteristics of newly discovered black smoker fluids and associated hydrothermal plumes at the Rodriguez Triple Junction, Central Indian Ridge. Earth and Planetary Science Letters, 193(3–4): 371–379, doi: 10.1016/S0012-821X(01)00511-8

Genna D, Gaboury D, Roy G. 2014. Evolution of a volcanogenic hydrothermal system recorded by the behavior of LREE and Eu: Case study of the Key Tuffite at Bracemac-McLeod deposits, Matagami, Canada. Ore Geology Reviews, 63: 160–177, doi: 10.1016/j.oregeorev.2014.04.019

German C R, Baker E T, Mevel C, et al. 1998. Hydrothermal activity along the Southwest Indian Ridge. Nature, 395(6701): 490–493, doi: 10.1038/26730

Halbach P, Blum N, Munch U, et al. 1998. Formation and decay of a modern massive sulfide deposit in the Indian Ocean. Mineralium Deposita, 33: 302–309, doi: 10.1007/s001260050149

Hannington M D, de Ronde C E J, Petersen S. 2005. Sea-floor tectonics and submarine hydrothermal systems. In: Hedenquist J W, Thompson J F H, Goldfarb R J, eds. Economic Geology 100th Anniversary Volume. Littleton, CO: Society of Economic Geologists, 111–141

Hannington M, Jamieson J, Monecke T, et al. 2011. The abundance of seafloor massive dulfide deposits. Geology, 39(12): 1155–1158, doi: 10.1130/G32468.1

Hannington M D, Tivey M K, Larocque A C L, et al. 1995. The occurrence of gold in sulfide deposits of the TAG hydrothermal field, Mid-Atlantic Ridge. The Canadian Mineralogist, 33: 1285–1310

Haymon R M. 1983. Growth history of hydrothermal black smoker chimneys. Nature, 301(5902): 695–698, doi: 10.1038/301695a0

Haymon R M, Kastner M. 1981. Hot spring deposits on the East Pacific Rise at 21°N: preliminary description of mineralogy and genesis. Earth and Planetary Science Letters, 53(3): 363–381, doi: 10.1016/0012-821X(81)90041-8

Hekinian R, Francheteaub J, Ballardc R D. 1985. Morphology and evolution of hydrothermal deposits at the axis of the East Pacific Rise. Oceanologica Acta, 8(2): 147–155

Herzig P M, Hannington M D. 1995. Polymetallic massive sulfides at the modern seafloor a review. Ore Geology Reviews, 10(2): 95–115, doi: 10.1016/0169-1368(95)00009-7

Jamieson J W, Hannington M D, Petersen S. 2017. Seafloor massive sulfide resources. In: Encyclopedia of Maritime and Offshore Engineering. Chichester: John Wiley & Sons

Jiang Zijing, Han Xiqiu, Wang Yejian, et al. 2015. Characteristics of hydrothermal anomalies in water bodies near Tianshui hydrothermal area of Karlsberg Ridge in the Northwest Indian Ocean. Acta Mineralogica Sinica (in Chinese), 35(S1): 765–766

Kelley D S, Baross J A, Delaney J R. 2002. Volcanoes, fluids, and life at mid-ocean ridge spreading centers. Annual Review of Earth and Planetary Sciences, 30: 385–491, doi: 10.1146/annurev.

earth.30.091201.141331
Kinsey J C, German C R. 2013. Sustained volcanically-hosted venting at ultraslow ridges: Piccard Hydrothermal Field, Mid-Cayman Rise. Earth and Planetary Science Letters, 380: 162–168, doi: 10.1016/j.epsl.2013.08.001
Koski R A, Jonasson I R, Kadko D C, et al. 1994. Compositions, growth mechanisms, and temporal relations of hydrothermal sulfide-sulfate-silica chimneys at the northern Cleft segment, Juan de Fuca Ridge. Journal of Geophysical Research: Solid Earth, 99(B3): 4813–4832, doi: 10.1029/93JB02871
Lim D, Kim J, Kim W, et al. 2022. Characterization of geochemistry in hydrothermal sediments from the newly discovered onnuri vent field in the middle region of the Central Indian Ridge. Frontiers in Marine Science, 9: 810949, doi: 10.3389/fmars.2022.810949
Ludwig K A, Kelley D S, Butterfield D A, et al. 2006. Formation and evolution of carbonate chimneys at the Lost City Hydrothermal Field. Geochimica et Cosmochimica Acta, 70(14): 3625–3645, doi: 10.1016/j.gca.2006.04.016
Münch U, Halbach P, Fujimoto H, et al. 2000. Sea-floor hydrothermal mineralization from the Mt. Jourdanne, Southwest Indian Ridge. JAMSTEC, 16: 125–132
Melchert B, Devey C W, German C R, et al. 2008. First evidence for high-temperature off-axis venting of deep crustal/mantle heat: The Nibelungen hydrothermal field, southern Mid-Atlantic Ridge. Earth and Planetary Science Letters, 275(1–2): 61–69, doi: 10.1016/j.epsl.2008.08.010
Meng Xingwei, Li Xiaohu, Chu Fengyou, et al. 2019. Multi-stage growth and fluid evolution of a hydrothermal sulphide chimney in the East Pacific Ridge 1–2°S hydrothermal field: constraints from *in situ* sulphur isotopes. Geological Magazine, 156(6): 989–1002, doi: 10.1017/S0016756818000316
Murton B J, Baker E T, Sands C M, et al. 2006. Detection of an unusually large hydrothermal event plume above the slow-spreading Carlsberg Ridge: NW Indian Ocean. Geophysical Research Letters, 33(10): L10608
Nakamura K, Morishita T, Bach W, et al. 2009. Serpentinized troctolites exposed near the Kairei Hydrothermal Field, Central Indian Ridge: Insights into the origin of the Kairei hydrothermal fluid supporting a unique microbial ecosystem. Earth & Planetary Science Letters, 280: 128–136
Olatunde P S, Akintoye A E. 2021. Integrated geochemical investigations on Fe-Mn nodules, polymetallic sulfides and Fe-Mn oxides recovered from marine sediments of Carlsberg Ridge, Northwest Indian Ocean. Advances in Environal Studies, 5(1): 394–403
Peng Xiaotong, Zhou Huaiyang. 2005. Growth history of hydrothermal chimneys at EPR 9–10°N: A structural and mineralogical study. Science in China Series D: Earth Sciences, 48(11): 1891–1899, doi: 10.1360/04yd0029
Petersen S, Kuhn K, Kuhn T, et al. 2009. The geological setting of the ultramafic-hosted Logatchev hydrothermal field (14°45′N, Mid-Atlantic Ridge) and its influence on massive sulfide formation. Lithos, 112(1–2): 40–56, doi: 10.1016/j.lithos.2009.02.008
Qiu Zhongyan, Han Xiqiu, Li Mou, et al. 2021. The temporal variability of hydrothermal activity of wocan hydrothermal field, Carlsberg Ridge, Northwest Indian Ocean. Ore Geology Reviews, 132: 103999, doi: 10.1016/j.oregeorev.2021.103999
Raju K A K, Chaubey A K, Amarnath D, et al. 2008. Morphotectonics of the Carlsberg Ridge between 62°20′ and 66°20E, Northwest Indian Ocean. Marine Geology, 252(3–4): 120–128, doi: 10.1016/j.margeo.2008.03.016
Robigou V, Delaney J R, Stakes D S. 1993. Large massive sulfide deposits in a newly discovered active hydrothermal system, the High-Rise field, Endeavour segment, Juan de Fuca Ridge. Geophysical Research Letters, 20(17): 1887–1890, doi: 10.1029/93GL01399
Sheng Mingwei, Tang Songqi, Cui Zhuang, et al. 2020. A joint framework for underwater sequence images stitching based on deep neural network convolutional neural network. International Journal of Advanced Robotic Systems, 17(2): 1–14
Tao Chunhui, Li Huaiming, Jin Xiaobing, et al. 2014. Seafloor hydrothermal activity and polymetallic sulfide exploration on the Southwest Indian Ridge. Chinese Science Bulletin, 59: 2266–2276
Tao Chunhui, Lin Jian, Guo Shiqin, et al. 2012. First active hydrothermal vents on an ultraslow-spreading center: Southwest Indian Ridge. Geology, 40(1): 47–50, doi: 10.1130/G32389.1
Tao Chunhui, Wu Guanghai, Deng Xianming, et al. 2013. New discovery of seafloor hydrothermal activity on the Indian Ocean Carlsberg Ridge and Southern North Atlantic Ridge—progress during the 26th Chinese COMRA cruise. Acta Oceanologica Sinica, 32(8): 85–88, doi: 10.1007/s13131-013-0345-x
Tivey M K. 2007. Generation of seafloor hydrothermal vent fluids and associated mineral deposits. Oceanography, 20(1): 50–65, doi: 10.5670/oceanog.2007.80
Tivey M K, Stakes D S, Cook T L, et al. 1999. A model for growth of steep-sided vent structures on the Endeavour Segment of the Juan de Fuca Ridge: Results of a petrologic and geochemical study. Journal of Geophysical Research: Solid Earth, 104(B10): 22859–22883, doi: 10.1029/1999JB900107
Van Dover C L, Humphris S E, Fornari D, et al. 2001. Biogeography and ecological setting of Indian Ocean hydrothermal vents. Science, 294(5543): 818–823, doi: 10.1126/science.1064574
Von Damm K L. 1995. Controls on the chemistry and temporal variability of seafloor hydrothermal fluids. In: Humphris S E, Zierenberg R A, Mullineaux L S, et al., eds. Seafloor Hydrothermal Systems: Physical, Chemical, Biological, and Geological Interactions. Washington, DC : American Geophysical Union, 222–247
Von Damm K L, Buttermore L G, Oosting S E, et al. 1997. Direct observation of the evolution of a seafloor 'black smoker' from vapor to brine. Earth and Planetary Science Letters, 149(1–4): 101–111, doi: 10.1016/S0012-821X(97)00059-9
Wang Yejian, Han Xiqiu, Petersen S, et al. 2018. Trace Metal Distribution in Sulfide Minerals from Ultramafic-Hosted Hydrothermal Systems: Examples from the Kairei Vent Field, Central Indian Ridge. Minerals, 8: 526
Wang Yejian, Han Xiqiu, Zhou Yadong, et al. 2021. The Daxi Vent Field: An active mafic-hosted hydrothermal system at a nontransform offset on the slow-spreading Carlsberg Ridge, 6°48′N. Ore Geology Reviews, 129: 103888, doi: 10.1016/j.oregeorev.2020.103888
Webber A P, Roberts S, Murton B J, et al. 2017. The formation of gold-rich seafloor sulfide deposits: Evidence from the Beebe hydrothermal vent field, Cayman Trough. Geochemistry, Geophysics, Geosystems, 18(6): 2011–2027
Wheeler A J, Murton B, Copley J, et al. 2013. Moytirra: Discovery of the first known deep-sea hydrothermal vent field on the slow-spreading Mid-Atlantic Ridge north of the Azores. Geochemistry, Geophysics, Geosystems, 14(10): 4170–4184
Yang Lei, Wang Xiangxin, Zhang Tongwei, et al. 2021b. Research on the application technology of manned submersible bathymetric sidescan sonar system in the abyss zone. In: 2021 OES China Ocean Acoustics. Harbin: IEEE, 293–298
Yang Ming, Wang Yejian, Han Xiqiu, et al. 2021a. Gold mineralization in the ultramafic-hosted seafloor hydrothermal systems: examples from the Tianxiu Vent Field, Carlsberg Ridge. Geological Review (in Chinese), 67(S1): 173–174
You Chenfeng, Bickle M J. 1998. Evolution of an active sea-floor massive sulphide deposit. Nature, 394(6694): 668–671, doi: 10.1038/29279
Yu Junyu, Tao Chunhui, Liao Shili, et al. 2021. Resource estimation of the sulfide-rich deposits of the Yuhuang-1 hydrothermal field on the ultraslow-spreading Southwest Indian Ridge. Ore Geology Reviews, 134: 104169, doi: 10.1016/j.oregeorev.2021.104169
Zhou Yadong, Chen Chong, Zhang Dongsheng, et al. 2022. Delineating biogeographic regions in Indian Ocean deep-sea vents and implications for conservation. Diversity and Distributions, 28(12): 2858–2870, doi: 10.1111/ddi.13535